

THE CALIFA AND HIPASS CIRCULAR VELOCITY FUNCTION FOR ALL MORPHOLOGICAL GALAXY TYPES

S. BEKERAITÉ¹, C.J. WALCHER¹, L. WISOTZKI¹, D.J. CROTON², J. FALCÓN-BARROSO^{3, 4}, M. LYUBENOVA⁵,
D. OBRESCHKOW⁶, S. F. SÁNCHEZ⁷, K. SPEKKENS⁸, P. TORREY^{9, 10}, G. VAN DE VEN¹¹, M.A. ZWAAN¹², Y. ASCASIBAR¹³,
J. BLAND-HAWTHORN¹⁴, R. GONZÁLEZ DELGADO¹⁵, B. HUSEMANN¹⁶, R.A. MARINO^{17, 18}, M. VOGELSBERGER¹⁹, B.
ZIEGLER²⁰

(Received May 11th; Revised July 22th; Accepted August 1st)

¹Leibniz-Institut für Astrophysik Potsdam (AIP), An der Sternwarte 16, D-14482 Potsdam, Germany

²Centre for Astrophysics and Supercomputing, Swinburne University of Technology, Hawthorn, Victoria 3122, Australia

³Dept. Astrofísica, Universidad de La Laguna, C/ Astrofísico Francisco Sánchez, E-38205-La Laguna, Tenerife, Spain

⁴Instituto de Astrofísica de Canarias, C/Vía Láctea S/N, 38200-La Laguna, Tenerife, Spain

⁵Kapteyn Astronomical Institute, University of Groningen, Postbus 800, 9700 AV Groningen, The Netherlands

⁶ICRAR, University of Western Australia, 35 Stirling Highway, Crawley, WA 6009, Australia

⁷Instituto de Astronomía, Universidad Nacional Autónoma de México, A.P. 70-264, 04510, México, D.F.

⁸Department of Physics, Royal Military College of Canada, P.O. Box 17000, Station Forces, Kingston, ON, K7K 7B4, Canada

⁹Department of Physics, Kavli Institute for Astrophysics and Space Research, Massachusetts Institute of Technology, Cambridge, MA 02139, USA

¹⁰TAPIR, Mailcode 350-17, California Institute of Technology, Pasadena, CA 91125, USA

¹¹Max Planck Institute for Astronomy, Königstuhl 17, D-69117 Heidelberg, Germany

¹²ESO, ALMA Regional Centre, Karl-Schwarzschild-Strasse 2, D-85748 Garching, Germany

¹³Departamento de Física Teórica, Facultad de Ciencias, Universidad Autónoma de Madrid, E-28049 Madrid, Spain

¹⁴Sydney Institute for Astronomy, School of Physics, University of Sydney, NSW 2006, Australia

¹⁵Instituto de Astrofísica de Andalucía (IAA/CSIC), Glorieta de la Astronomía s/n Aptdo. 3004, E-18080 Granada, Spain

¹⁶European Southern Observatory, Karl-Schwarzschild-Str. 2, D-85748 Garching b. München, Germany

¹⁷Department of Physics, Institute for Astronomy, ETH Zürich, CH-8093 Zürich, Switzerland

¹⁸Departamento de Astrofísica y CC. de la Atmósfera, Facultad de CC. Físicas, Universidad Complutense de Madrid, Avda. Complutense s/n, 28040 Madrid, Spain

¹⁹Department of Physics, Kavli Institute for Astrophysics and Space Research, Massachusetts Institute of Technology, Cambridge, MA 02139, USA

²⁰University of Vienna, Türkenschanzstr. 17, 1180 Vienna, Austria

ABSTRACT

The velocity function is a fundamental observable statistic of the galaxy population, similarly important as the luminosity function, but much more difficult to measure. In this work we present the first directly measured circular velocity function that is representative between $60 < v_{\text{circ}} < 320 \text{ km s}^{-1}$ for galaxies of all morphological types at a given rotation velocity. For the low mass galaxy population ($60 < v_{\text{circ}} < 170 \text{ km s}^{-1}$), we use the HIPASS velocity function. For the massive galaxy population ($170 < v_{\text{circ}} < 320 \text{ km s}^{-1}$), we use stellar circular velocities from the Calar Alto Legacy Integral Field Area Survey (CALIFA). In earlier work we obtained the measurements of circular velocity at the 80% light radius for 226 galaxies and demonstrated that the CALIFA sample can produce volume-corrected galaxy distribution functions. The CALIFA velocity function includes homogeneous velocity measurements of both late and early-type rotation-supported galaxies and has the crucial advantage of not missing gas-poor massive ellipticals that HI surveys are blind to. We show that both velocity functions can be combined in a seamless manner, as their ranges of validity overlap. The resulting observed velocity function is compared to velocity functions derived from cosmological simulations of the $z = 0$ galaxy population. We find that dark matter-only simulations show a strong mismatch with the observed VF. Hydrodynamic simulations fare better, but still do not fully reproduce observations.

Keywords: Galaxies: kinematics and dynamics — galaxies: statistics — galaxies: evolution

1. INTRODUCTION

The circular velocity function (VF), the space density of galaxies as a function of their circular rotation velocities, is directly related to total dynamical masses of the galaxies and not dominated by their baryonic content, unlike the galaxy luminosity function (LF) (Desai et al. 2004). As a tracer of dark matter halo masses (Zwaan et al. 2010, hereafter Z10), the VF can be used as a test of the Λ CDM paradigm (Klypin et al. 2015; Papastergis et al. 2011) and a probe of cosmological parameters (Newman & Davis 2000, 2002) or the relation between the dark matter halo and galaxy rotation velocities.

Observationally, VF differs significantly from the LF. The latter, although difficult to predict and interpret theoretically, is much easier to measure (Klypin et al. 2015) and does not depend on the spatial distribution of baryons in galaxies. Depending on the precise definition of circular velocity, the VF is a function of both the halo and baryonic mass spatial distribution and their ratio in a particular galaxy, however, it is not significantly affected by uncertainties in the stellar mass-to-light ratio. In this regard it is a superior tool for testing the results of cosmological simulations.

Measuring the VF is difficult on all halo mass scales. Cluster rotation velocities have completely different dynamical properties and require different observational methods than individual galaxies (Kochanek & White 2001), while the lowest velocity galaxy samples are not complete. Even at intermediate velocities the VF has not been fully constrained, because circular velocity measurements for gas-poor early-types, dominating the high velocity end of the galaxy velocity function, are notoriously challenging (Gonzalez et al. 2000; Papastergis et al. 2011; Obreschkow et al. 2013). Moreover, even though the circular velocity is easy to define theoretically, there is no clear observational definition, especially given that the rotation curves of some classes of galaxies do not flatten.

Several studies have attempted to use galaxy scaling relations in order to infer circular velocities from more accessible observable quantities. Gonzalez et al. (2000) estimate a VF by converting the SSRS2 luminosity function using the Tully-Fisher relation. A similar approach was adopted by Abramson et al. (2014), who construct galaxy group and field VFs using velocity estimates based on Sloan Digital Sky Survey (SDSS) photometric data. Desai et al. (2004) construct cluster and field VFs by using SDSS data, Tully-Fisher and Fundamental Plane relations.

In Klypin et al. (2015) a Local Volume VF, complete

down to $v_{\text{circ}} \approx 15 \text{ km s}^{-1}$, was estimated using a combination of HI observations and line-of-sight velocities estimated from photometry. However, their study does not sample the velocities above $\approx 200 \text{ km s}^{-1}$.

An HI velocity function down to 30 km s^{-1} was directly measured from HI Parkes All Sky Survey (HIPASS) linewidths (Z10). Nevertheless, as shown in Obreschkow et al. (2013), massive, rapidly rotating, gas-poor ellipticals are systematically missing from HIPASS data. Therefore its high velocity end is very incomplete.

Papastergis et al. (2011) (P11) estimate the HI linewidth function from Arecibo Legacy Fast ALFA (ALFALFA) survey data and suggest using the linewidth function as a more useful probe of the halo mass distribution. They also provide a VF for all types by combining their VF with the velocity function converted from Chae (2010) velocity dispersion measurements.

CALIFA is in a unique position with its well-understood selection function, a wide field of view and the first IFS sample that includes a large number of galaxies with diverse morphologies. As described in Krajinović et al. (2008), 80% of early-type galaxies can be expected to have a rotating component. The use of stellar kinematics enables us to include gas-poor, rotating early-type galaxies in a homogeneous manner. Therefore we are able to directly measure the VF for rotating galaxies of all morphological types, in contrast to the inferred VFs reported by Gonzalez et al. (2000); Desai et al. (2004); Chae (2010); Abramson et al. (2014).

Within this work, we assume a benchmark cosmological model with $H_0 = 70 \text{ km s}^{-1}/\text{Mpc}$, $\Omega_\Lambda = 0.7$ and $\Omega_M = 0.3$. All VFs from the literature were rescaled to this particular cosmology, as described in Croton (2013).

2. CALIFA STELLAR CIRCULAR VELOCITY MEASUREMENTS

CALIFA observations use the PMAS instrument (Roth et al. 2005) in PPaK (Verheijen et al. 2004) mode, mounted on the 3.5 m telescope at the Calar Alto observatory. The CALIFA survey, sample and data analysis pipeline are described in detail Sánchez et al. (2012); Husemann et al. (2013); García-Benito et al. (2015); Walcher et al. (2014). We refer the reader to the first paper of the CALIFA stellar kinematics series (Falcón-Barroso et al., submitted) where the kinematic map extraction and sample is described in full detail.

In this analysis, we use the "useful" galaxy sample defined in Bekeraité et al. (2016, B16) and the circular velocity measurements obtained therein. Briefly, we start with the initial statistically complete sample of 277 available stellar velocity fields, 51 of which were not use-

ful for further analysis due to S/N issues (low number of Voronoi bins, foreground contamination) or extremely distorted velocity fields. The final sample consisted of 226 galaxies. As shown in B16, the rejected galaxies were predominantly fainter (SDSS $M_r > -20$ mag), which affected the lower completeness limit but did not introduce bias in the sample above it.

We then fit the position and rotation curve parameters by performing Markov Chain Monte Carlo (MCMC) modelling of the velocity fields. The rotation velocity v_{opt} was estimated by evaluating the model rotation velocity at the 80% light radius (the optical radius). Due to CALIFA’s large but still limited field of view rotation curve extrapolation was necessary for 165 galaxies.

We do not split the galaxy sample into ellipticals and spirals to estimate their v_{circ} values separately. Instead, as described in Sec. 4.4 of B16, a correction estimated in Kalinova et al. (submitted) has been applied to all galaxies. Kalinova et al. (submitted) analyse the relationship between dynamical masses inferred using the classical ADC approach (see Chapter 4, Binney & Tremaine 2008) and axisymmetric Jeans anisotropic Multi-Gaussian (JAM) models applied to stellar mean velocity and velocity dispersion fields of 18 late-type galaxies observed with the SAURON IFS instrument. We utilise the relation provided in their Table 4 and calculate the circular velocities by multiplying the measured velocity by the square root of the factors provided, based on the ratio between the v_{opt} and the line-of-sight stellar velocity dispersion at the optical radius. We demonstrate that the obtained circular velocity is comparable with ionised gas rotation velocity in B16.

3. RESULTS

3.1. CALIFA circular velocity function

We measure the CALIFA stellar circular VF Ψ_{circ} in the same manner as the LFs in Walcher et al. (2014, W14) and B16, estimating the optimal number of velocity bins using Scott’s Rule (Scott 1979). The $1/V_{\text{max}}$ weights, corrected for cosmic variance as described in W14 are assigned to each galaxy and then used to calculate the VF. We note that the uncertainties correspond to Poissonian errors in each bin only and do not include any uncertainties in circular velocity measurements see Sec. 3.2.

As can be seen in Fig.1, the high-velocity end of Ψ_{circ} lies significantly above the Z10 or P11 HI velocity functions. This was to be expected since HI surveys are blind to gas-poor massive ellipticals (Obreschkow et al. 2013). However, the CALIFA VF is below the higher-velocity end of P11 inferred VF for all galaxy types. This is not surprising given that their VF combines the observed ALFALFA VF and the velocity dispersion function of

Chae (2010). Our circular VF is defined for rotation-dominated galaxies only and we do not include the velocity dispersion contribution in any way, barring the circular velocity correction described in Sec. 2.

At lower velocities the CALIFA VF starts to fall off rapidly and deviates from the Schechter function shape. We estimate the region where incompleteness should become important, based on the luminosity function of the sample provided in B16. We convert the luminosity completeness limits to velocity using the Tully-Fisher relation measured in B16 and find that the CALIFA VF should be complete within the velocity range of $140 < v_{\text{circ}} < 345 \text{ km s}^{-1}$. Such a direct conversion excludes the scatter in TFR, which causes a fall-off sooner than would be naively expected from the TFR alone. By taking the *rms* TFR scatter (0.27 mag) into account, we find that the CALIFA velocity function, as shown in Fig.1, can be safely assumed to be complete above 170 km s^{-1} . At the high velocity end, the CALIFA survey is limited by its survey volume as the total number of galaxies brighter than $M_r = -23$ expected within the survey is of the order of unity. Given the low number of galaxies at the high velocity end of the TFR, we are unable to estimate the real TFR scatter among the most massive galaxies and the subsequent onset of bias. However, conservatively adopting the *rms* TFR scatter of 0.27 mag we find that the CALIFA VF is complete at least up to 320 km s^{-1} .

3.2. Uncertainties

The CALIFA stellar rotation velocity measurements have significant uncertainties, resulting from limited spatial resolution of binned stellar velocity fields, limited CALIFA field of view and pressure-support dependent correction term. The circular VF is likely affected by all these factors. A broader discussion of uncertainties in the circular velocity measurements and volume correction weights is contained in B16 and W14.

In order to check the impact of velocity measurement uncertainties we employ a resampling method similar to P11. We generate 200 mock CALIFA VF samples (shown in Fig. 2) in which the volume weights are not changed, but the velocities v_{circ} are replaced with randomly drawn values such that $v_{\text{circ}}^{\text{test}} = v_{\text{circ}} + \mathcal{N}(0, \sigma_v)$, where σ_v are the individual velocity uncertainties of each point.

Overall, the effect is a smoothing of the VF as the datapoints are ‘smeared’ into the neighbouring bins. As the $1/V_{\text{max}}$ weights are higher at the lower velocities, this leads to an artificial boost at the highest velocity end. Undoubtedly, this effect should be present in our VF as well, making the location of the highest velocity CALIFA datapoint even more uncertain. Given that this bin only includes 3 galaxies and is outside our esti-

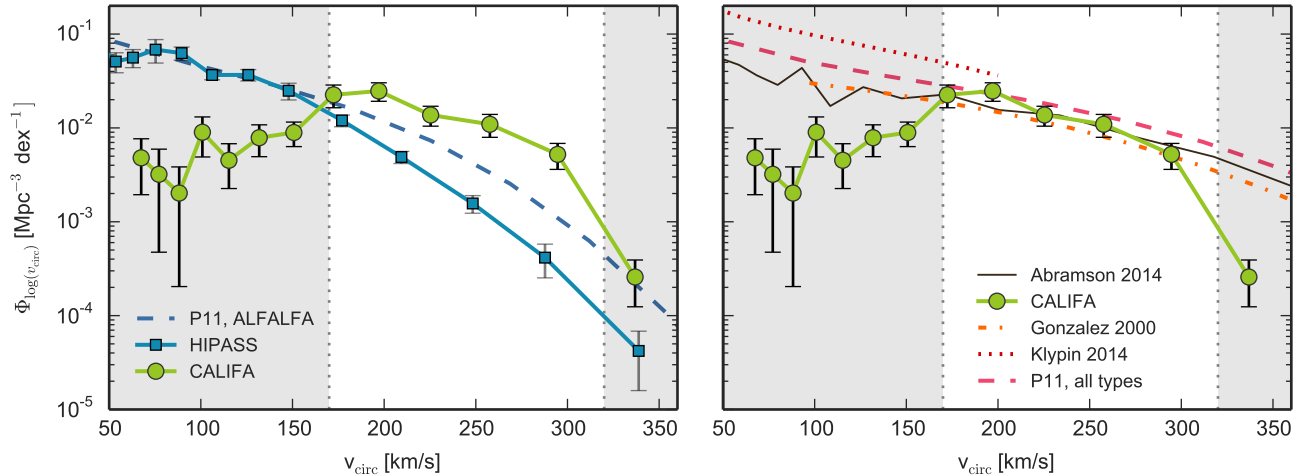


Figure 1. CALIFA velocity function, compared with the HIPASS (Z10), Gonzalez et al. (2000); Klypin et al. (2015); Abramson et al. (2014) and P11 measurements. The left panel shows the comparison with the observed VFs of rotation-dominated gas-rich galaxies. The right panel displays the comparison with indirectly estimated VFs. The shaded areas and dotted vertical lines show an approximate region where incompleteness in the CALIFA sample becomes important.

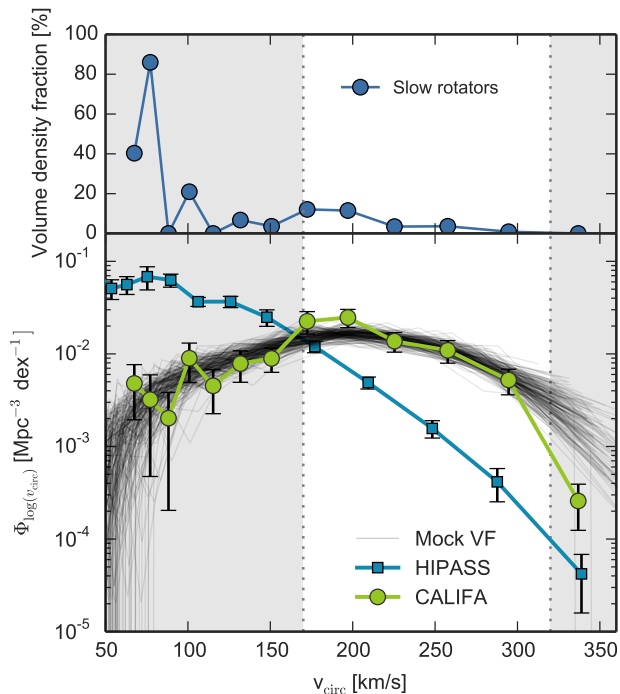


Figure 2. Top panel shows the volume density fraction of slow rotators (SR), for which the measured rotation velocities and circular velocity corrections are the most uncertain. This fraction does not reach 20% of volume density at for $v_{\text{circ}} \gtrsim 110 \text{ km s}^{-1}$. Bottom panel shows the effect of velocity measurement uncertainties on the velocity function. Thin grey lines are the mock realisations of the VF. The green points and line are the CALIFA VF. The blue line shows the HIPASS VF.

mated completeness range, we exclude it from all further analysis.

Table 1. Schechter function fit parameters for CALIFA+HIPASS VF (Eq.1).

$\Psi_* [\times 10^{-3} \text{ Mpc}^{-3}]$	$v_* [\text{km s}^{-1}]$	α
130.0 ± 35.8	89.3 ± 32.8	0.2 ± 0.6

3.3. Combined CALIFA-HIPASS circular velocity function

In order to extend the VF to a wider velocity range we merge the HIPASS VF between $60\text{--}160 \text{ km s}^{-1}$ and CALIFA circular velocities between $160\text{--}320 \text{ km s}^{-1}$, effectively choosing the more complete VF in each bin. Merging the two VFs in this way is justified as HI-rich late-type galaxies dominate the counts below 200 km s^{-1} . At the high mass limit, early-type massive rotators contribute significantly to the high velocity end, where the CALIFA sample is expected to be complete at least up to $v_{\text{circ}} = 320 \text{ km s}^{-1}$, as described above.

We fit a Schechter function

$$\Psi(v_{\text{circ}}) = \Psi_* \left(\frac{v_{\text{circ}}}{v_*} \right)^\alpha \exp \left[- \left(\frac{v_{\text{circ}}}{v_*} \right) \right] \quad (1)$$

to the combined VF, shown in Fig. 3. The datapoints are listed in Table 2 and the fit parameters are provided in Table 1. Uncertainties for the HIPASS values were taken from Obreschkow et al. (2013), where they supplement direct measurement and shot noise with other uncertainties such as distance errors, cosmology uncertainties and cosmic variance. Similarly to Z10, we find that the model parameters are highly covariant.

3.4. Discussion

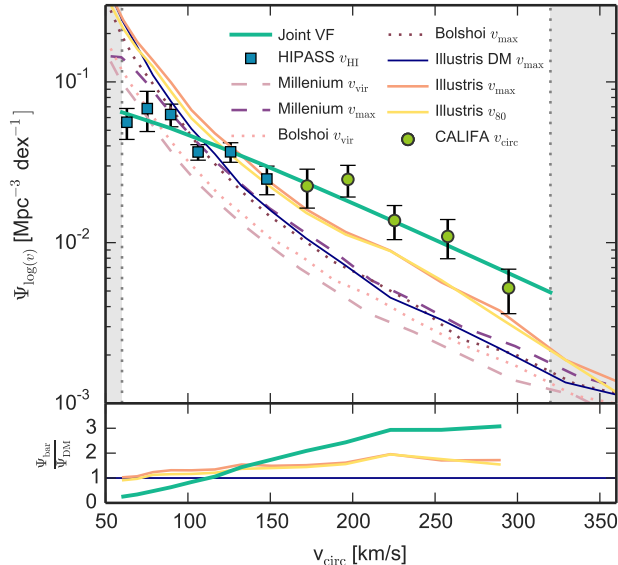


Figure 3. Zoomed-in view showing the combined CALIFA+HIPASS VF and the best Schechter fit, shown as thick solid teal line. In the top panel, dark matter-only halo VFs from Millenium and Bolshoi simulations are shown as purple and pink dashed and dotted lines. v_{max} VF from Illustris-1 dark-matter only simulation is shown by a thin dark blue line. Full-physics Illustris-1 simulation VFs, calculated using the subhalo v_{max} and circular velocity at 80% stellar mass radius (v_{80}) are displayed as orange and yellow solid lines respectively. The lower panel shows the ratio between the baryonic simulated VFs, the combined CALIFA+HIPASS fit and the DM-only Illustris VF. See Sec. 3.5 for a description, discussion, and references.

Table 2. CALIFA-HIPASS velocity function values.

Survey	v_{circ} [km s^{-1}]	$\Psi(\log_{10} v_{\text{circ}})$ [$\times 10^{-3} \text{Mpc}^{-3}$]
HIPASS	63.0	56.1 ± 12.2
	75.3	68.2 ± 19.1
	89.5	62.7 ± 10.1
	106.2	36.6 ± 4.1
	125.9	36.7 ± 5.1
	147.9	24.9 ± 5.0
CALIFA	172.4	22.5 ± 6.1
	197.1	24.7 ± 5.5
	225.4	13.7 ± 3.3
	257.7	10.9 ± 3.0
	294.6	5.2 ± 1.6

Despite the care with which we have undertaken our analysis, combining the HI rotation velocities and stellar circular rotation velocities as we have done has some caveats.

First of all, the actual methods used to construct the HIPASS and CALIFA VFs are different. The CALIFA volume correction procedure uses a more straightforward $1/V_{\text{max}}$ method (Schmidt 1968) improved by ac-

counting for the radial density variations.

Meanwhile, Z10 employ a bivariate step-wise maximum likelihood (2DSWML) technique to obtain their space densities. Zwaan et al. (2003) verify that the method is insensitive to even large radial density variations. In addition, the HIPASS linewidth function (WF) matches the WF obtained from the deeper ALFALFA survey down to 60 km s^{-1} (P11), confirming that the effect of large scale structure on the HIPASS VF is negligible, at least in the range of our analysis. As shown in Zwaan et al. (2003), the $1/V_{\text{max}}$ and 2DSWML methods yield practically indistinguishable results, confirming that the two VFs derived using both methods are compatible.

The HIPASS sample consists of late-type galaxies only, since visually classified early-type galaxies, comprising 11% of the sample, have been removed. However, the fraction of early-type and S0 galaxies is reported to only have a noticeable effect on the VF only for galaxies with rotation velocities above 200 km s^{-1} , where we use CALIFA VF values already.

HIPASS linewidths have been corrected for inclination using SuperCOSMOS imaging b -band photometric axis ratios (Meyer et al. 2008), while we use kinematic inclinations obtained from MCMC modelling of the 2D velocity fields. Photometric inclination estimates are systematically affected by unknown intrinsic disk thickness, choice of b/a measurement radius and any departure from a perfect circular disk shape. However, given that Z10 exclude galaxies with estimated inclinations $i < 45^\circ$ due to larger uncertainties at low inclinations, inconsistencies in inclination measurements are unlikely to have had a significant effect.

As discussed in Z10, HIPASS may not detect HI at the flat part of the rotation curve for all galaxies, especially those with $v_{\text{circ}} \leq 60 \text{ km s}^{-1}$. Similarly, a small fraction of low-mass galaxies might not have enough gas to have been detected by HIPASS. We treat the lowest VF end with caution, and exclude HIPASS datapoints below 60 km s^{-1} from the combined fit. Therefore, the joint velocity function should be representative in the velocity range of $60 < v_{\text{circ}} < 320 \text{ km s}^{-1}$.

3.5. Comparison with simulations

We compare our work with a number of simulations. Shown in Fig. 3 are the VFs from the Millennium (Springel et al. 2005) and Bolshoi (Klypin et al. 2011) dark matter simulations. Here we are plotting friends-of-friends DM halos using two different halo circular velocity definitions: virial velocity v_{vir} and maximum circular velocity v_{max} . In addition, we show the Illustris-1 DM-only run v_{max} -based VF, constructed for haloes with $M_{\text{DM}} > 10^{10} M_{\odot}$.

We also include two VFs measured from Illustris-1

full-physics simulations (Vogelsberger et al. 2014b,a). Illustris v_{\max} is calculated for all subhaloes with stellar masses $M_* > 10^8 M_\odot$, while Illustris v_{80} is calculated as the gravitational potential-induced circular rotation velocity at the 80% stellar mass radius.

It is strikingly evident that the observed VF does not agree with the dark matter-only simulations, even though the low velocity end of Bolshoi and Millenium simulations displays marginal agreement with the observational data. At intermediate velocities the dark matter-only VFs sit well below both the observed data and the baryonic simulation.

However, we find that the observed VF cannot be reconciled with the Illustris v_{80} and v_{\max} -based VFs, though the full physics simulations produce VFs that are significantly closer to the observed VF. The lack of observed galaxies is evident for velocities lower than $v_{\text{circ}} \approx 120 \text{ km s}^{-1}$. This fact was already shown in Gonzalez et al. (2000); Papastergis et al. (2011); Abramson et al. (2014) and Z10, however, we find it worthy to revisit their results using the latest hydrodynamical simulation results.

Interestingly, at the intermediate velocities the predicted VFs are systematically offset from the observations, differing by up to a factor of 3. This discrepancy is not related to the "under-abundance" problem.

The mismatch between simulations and observations is either a result of an inconsistency in the way that observations and simulations are measuring the velocity function, or the structure of simulated galaxies is inconsistent with the structure of observed galaxies. We have not yet performed a fully fair comparison between the simulations and observations using the 80% light radius in both cases, employing adequate surface brightness cuts and including projection effects for the simulation. In the very recent paper by Macciò et al. (2016) it was shown that at least some of the tension between the data and models at the low end of the velocity function can be alleviated by considering finite extent of HI disks and relatively larger vertical velocity dispersion. Observational confirmation of their result would go a long way towards explaining the tension in the VF comparison at low circular velocities. We additionally note that while the Illustris VF does not fully match the observed data at high circular velocities, further study of the effects of baryons on the masses and structure of dark matter halos may close the remaining gap. The difference between observed and simulated VF should be considered to be a constraint on the future generations of galaxy formation models.

4. CONCLUSIONS

In this work we measure the CALIFA stellar VF, derived from a sample of 226 stellar velocity fields. To our

best knowledge, it is the first directly measured VF that includes early-type fast rotators as well as late-types.

We then combined this VF with the HIPASS VF to obtain the first directly measured velocity function that simultaneously covers a wide range of circular velocities and morphological types. This has the benefit of using the space density and velocity data measured from the same surveys, without assuming scaling relations or conversions between kinematic observables. The combined VF is complete in the range of $60 < v_{\text{circ}} < 320 \text{ km s}^{-1}$. We find that Illustris simulation VF does not reproduce the observed data in both the low and high velocity ranges.

The differences between Λ CDM predictions and the observed VF are not so dissimilar to those found when comparing the halo and stellar mass functions. There, physical processes important for galaxy formation cause a decoupling of the halo and galaxy growth. By highlighting similar discrepancies, this work opens a new window for comparison with theory that should deepen our understanding of galaxy evolution. The resulting velocity function is expected to provide constraints on galaxy assembly and evolution models, insights into baryonic angular momentum, help improve halo occupation distribution and semi-analytic disk formation models.

The authors would like to express gratitude to Louis Abramson for kindly providing their VF data and for assistance with interpreting it. We sincerely thank the referee for the insightful comments.

SB acknowledges support from BMBF through the Erasmus-F project (grant number 05 A12BA1) and is grateful to Leibniz-Institut für Astrophysik Potsdam for its hospitality during her guest stay there in 2016. JFB acknowledges support from grant AYA2013-48226-C3-1-P from the Spanish Ministry of Economy and Competitiveness (MINECO). CJW acknowledges support through the Marie Curie Career Integration Grant 303912. SFS thanks the CONACYT-125180 and DGAPA-IA100815 projects for providing him support in this study. DO thanks the University of Western Australia for its support via a Research Collaboration Award. KS acknowledges funding from the Natural Sciences and Engineering Research Council of Canada.

This study makes use of the data provided by the Calar Alto Legacy Integral Field Area (CALIFA) survey (<http://www.califa.caha.es>). Based on observations collected at the Centro Astronómico Hispano Alemán (CAHA) at Calar Alto, operated jointly by the Max-Planck-Institut für Astronomie and the Instituto de Astrofísica de Andalucía (CSIC). CALIFA is the first legacy survey being performed at Calar Alto.

We have extensively used open source data analysis and visualisation tools *Matplotlib* (Hunter 2007) and

SciPy (Jones et al. 2001-2015).

REFERENCES

- Abramson, L. E., Williams, R. J., Benson, A. J., Kollmeier, J. A., & Mulchaey, J. S. 2014, *ApJ*, 793, 49
- Bekeraite, S., Walcher, J., & Falcón-Barroso, J. 2016, *ApJ*, accepted
- Binney, J., & Tremaine, S. 2008, *Galactic Dynamics: Second Edition* (Princeton University Press)
- Chae, K.-H. 2010, *MNRAS*, 402, 2031
- Croton, D. J. 2013, *PASA*, 30, 52
- Desai, V., Dalcanton, J. J., Mayer, L., et al. 2004, *MNRAS*, 351, 265
- García-Benito, R., Zibetti, S., Sánchez, S. F., et al. 2015, *A&A*, 576, A135
- Gonzalez, A. H., Williams, K. A., Bullock, J. S., Kolatt, T. S., & Primack, J. R. 2000, *ApJ*, 528, 145
- Hunter, J. D. 2007, *Computing In Science & Engineering*, 9, 90
- Husemann, B., Jahnke, K., Sánchez, S. F., et al. 2013, *A&A*, 549, A87
- Jones, E., Oliphant, T., Peterson, P., et al. 2001-2015, *SciPy: Open source scientific tools for Python*, , [Online; accessed 2015-06-17]
- Kalinova, V., van de Ven, G., Lyubenova, M., Falcón-Barroso, J., & et al. submitted, *MNRAS*
- Klypin, A., Karachentsev, I., Makarov, D., & Nasonova, O. 2015, *MNRAS*, 454, 1798
- Klypin, A. A., Trujillo-Gomez, S., & Primack, J. 2011, *ApJ*, 740, 102
- Kochanek, C. S., & White, M. 2001, *ApJ*, 559, 531
- Krajnović, D., Bacon, R., Cappellari, M., et al. 2008, *MNRAS*, 390, 93
- Macciò, A. V., Udrescu, S. M., Dutton, A. A., et al. 2016, *ArXiv e-prints*, arXiv:1607.01028
- Meyer, M. J., Zwaan, M. A., Webster, R. L., Schneider, S., & Staveley-Smith, L. 2008, *MNRAS*, 391, 1712
- Newman, J. A., & Davis, M. 2000, *ApJL*, 534, L11
- . 2002, *ApJ*, 564, 567
- Obreschkow, D., Ma, X., Meyer, M., et al. 2013, *ApJ*, 766, 137
- Papastergis, E., Martin, A. M., Giovanelli, R., & Haynes, M. P. 2011, *ApJ*, 739, 38
- Roth, M. M., Kelz, A., Fechner, T., et al. 2005, *PASP*, 117, 620
- Sánchez, S. F., Kennicutt, R. C., Gil de Paz, A., et al. 2012, *A&A*, 538, A8
- Schmidt, M. 1968, *ApJ*, 151, 393
- Scott, D. W. 1979, *Biometrika*, 66, pp. 605
- Springel, V., White, S. D. M., Jenkins, A., et al. 2005, *Nature*, 435, 629
- Verheijen, M. A. W., Bershady, M. A., Andersen, D. R., et al. 2004, *Astronomische Nachrichten*, 325, 151
- Vogelsberger, M., Genel, S., Springel, V., et al. 2014a, *MNRAS*, 444, 1518
- . 2014b, *Nature*, 509, 177
- Walcher, C. J., Wisotzki, L., Bekeraite, S., et al. 2014, *A&A*, 569, A1
- Zwaan, M. A., Meyer, M. J., & Staveley-Smith, L. 2010, *MNRAS*, 403, 1969
- Zwaan, M. A., Staveley-Smith, L., Koribalski, B. S., et al. 2003, *AJ*, 125, 2842